PAPER • OPEN ACCESS

An Investigation on Chemical Machining of NiTi SMA Prepared by Powder Metallurgy

To cite this article: Haydar Al-Ethari *et al* 2019 *IOP Conf. Ser.: Mater. Sci. Eng.* **518** 032032

View the article online for updates and enhancements.

IOP ebooks™

Bringing you innovative digital publishing with leading voices to create your essential collection of books in STEM research.

Start exploring the collection - download the first chapter of every title for free.

This content was downloaded from IP address 180.76.149.31 on 20/09/2019 at 09:07

IOP Conf. Series: Materials Science and Engineering **518** (2019) 032032 doi:10.1088/1757-899X/518/3/032032

An Investigation on Chemical Machining of NiTi SMA Prepared by Powder Metallurgy

Haydar Al-Ethari[1], Ali Hubi Haleem[1], Noora Mohammed Gased[2]

[1]University of Babylon, dralethariah@yahoo.com, alialihhhobi@yahoo.com
[2]University of Qadisiyah, nooraqased@gmail.com

Abstract. Chemical machining is very important in solving problems constantly arising due to the requirement of high surface finish along with high productivity through machining of metals and alloys. Such requirement appears in machining of NiTi shape memory alloy (55wt%Ni and 45wt% Ti) which has widespread engineering applications. The present work aimed at utilizing of Taguchi design of experiments with the method of desirability function to optimize the chemical machining parameters (machining temperature and machining time) of NiTi alloy prepared by powder metallurgy technique. Taguchi experimental design concept, L25 (2×5) orthogonal array was used to determine the S/N ratio. Based on the analyses of multiple regression method, mathematical predictive models for the studied parameters had designed and validated. To achieve the objectives of the present work Datafit ver9, and Mini Tab14 softwares had employed. The powders with the required percentages were mixed for 5hours, compacted at pressure of 900MPa, and sintered in two stages, at 500°C for 2 hours and then at 950°C for 6hours under vacuum conditions (10-4 torr). The X-ray diffraction test showed that the prepared sample are consisting of three phases (NiTi monoclinic phase, NiTi cubic phase, and Ni3Ti hexagonal phase). Machining temperature appears as the most significant factor, which controls both surface roughness and metal removal rate. Two mathematical models were developed to predict the metal removal rate and the surface roughness for any collection of machining temperature, and machining time. A minimum surface roughness of 0.666μm with a maximum metal removal rate of 0.0041g/min can be associated with machining temperature of 650C and machining time of 2min in solution consisting of 6%HCl, 19%HNO_3, and 75%H_2O.

1. Introduction

Shape memory alloys (SMA) are characterized by special properties in comparison with conventional metals. This type of alloys is a smart material that has the ability to return to its pre-deformed size and shape upon being subjected to an appropriate heat treatment. In addition to the shape memory effect, such alloys are capable of displaying pseudoelasticity giving the material the ability to transform between phases upon loading and unloading and recover to its original zero strain shape after significant deformation. With the properties such as repeatability, wear resistance, corrosion resistance and biocompatibility, NiTi alloy (also called nitinol) is the most commercially successful SMA [1]. Such alloy is composed of 55wt% Ni and 45wt% Ti. The shape memory and pseudoelastic characteristics coupled with the biocompatibility of this alloy make it an attractive candidate for medical applications [2]. Nitinol alloys are very difficult to machine by traditional machining methods. This difficulty arises because this type of alloys has more of the characteristics of titanium than of nickel, so heat generated during machining is not discharged smoothly. This leads to internal stresses, which causes negative effects on the SME of these alloys [3]. The poor chip breaking and the formation of burrs due to the remarkable high ductility of NiTi alloys are serious problems in turning these materials. Drilling causes an increase of the micro hardness in the subsurface zone of the workpeice. This influences the shape

Content from this work may be used under the terms of the Creative Commons Attribution 3.0 licence. Any further distribution of this work must maintain attribution to the author(s) and the title of the work, journal citation and DOI.
Published under licence by IOP Publishing Ltd

memory properties of the machined alloy [4, 5]. Higher tool wear, and poor surface finish are further limits to use the conventional methods in machining the SMA. As a result, to all these difficulties, various non-traditional machining methods are suggested to machine nitinol.

Huang and his coworkers used micro EDM with ultrasonic vibration for fabricating microholes in nitinol [6]. Chengde and his coworkers [7] studied femtosecond laser processing of NiTi SMA. Pfeifer and his coworkers investigated the influence of process parameters of pulsed Nd:YAG laser cutting of NiTi shape memory alloys [8]. Lee and Shin to the machining of nitinol [3] applied electrochemical polishing. Muhammad and his coworkers [9] presented picosecond laser micromachining of nitinol and platinum–iridium alloy for coronary stent applications. Abidi et al investigated the micro-electrical discharge machining of nickel-titanium shape memory alloy using grey relations coupled with principal component analysis [10].

The powder metallurgy (P/M) process is a near-net or net-shape manufacturing process with the development of final designed physical and mechanical properties. Powder metal parts needs machining processes but in limited scales to get a desired surface finish and close tolerances. Thus, the powder metallurgy process was used to prepare all samples of the present work.

It is essential to choose the machining method properly specially for finishing processes of parts produced by powder metallurgy technique. Chemical machining (CHM) can easily and successfully used for machining parts with complex and difficult to machine geometry without any side effects on their mechanical and physical properties. This process is a precision contouring of metal into any size, and shape without use of physical force, by a controlled chemical reaction. Material can remove by microscopic electrochemical cell action, as occurs in corrosion or chemical dissolution of a metal [11]. Several parameters affect the performance of the chemical machining process, the more important of which are: the type of etchant solution and its concentration, the maskant and its application, machining temperature, machining time, and the previous conditions of the part to machine. Such parameters have direct effect on the machining processes and on the characteristics of the machined parts concerning the machining rate, production tolerance, and particularly the surface finish [12]. There appear to need an investigation to determine the optimum conditions of the affecting parameters in order to enhance the performance of the CHM process used for machining Nitinol produced by powder metallurgy technique.

The objective of the present work aimed at investigating the influence of machining temperature, and machining time on surface finish and metal removal rate (MRR) of Nitinol prepared by powder metallurgy technique.

Taguchi experimental design concept, L25 (2×5) orthogonal array, was used in this investigation. Significant parameter affecting the surface finish and MRR was indicated based on S/N ratio. To optimize the process parameters the method of desirability function was used. Based on the analyses of multiple regression method, mathematical predictive models had designed and validated to select a combination of the studied parameters. To achieve the analyses of the present work Datafit ver9, and Mini Tab14 softwares had employed.

2. Powders used in this Investigation:

Samples of NiTi (55wt%Ni and 45wt%Ti) were prepared by using powder metallurgy technique. The particle size for Ni and Ti powders was tested by using laser particle size analyzer [model: better size 2000]. Figure 1 shows that the average size of the used powders was 12.08 µm for Ti and 36.80µm for Ni.

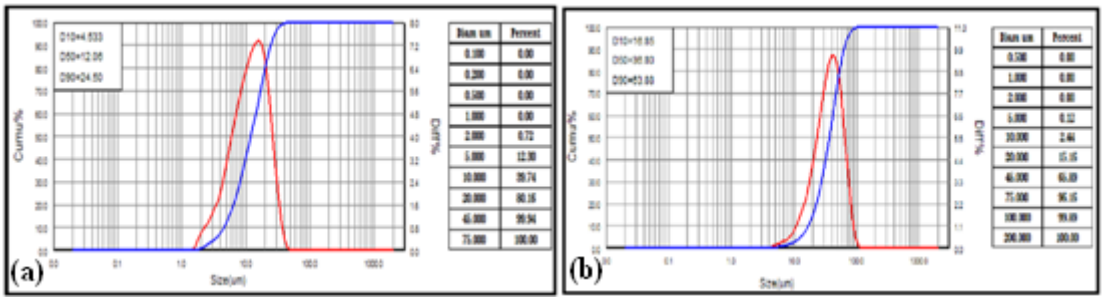

Figure 1. Particle Size Distribution of: (a) Ti Powder: (b) Ni Powder

3. Samples Preparation:

A wet mixing process was used for 5 hours. An electrical rolling mixer with stainless steel balls of different diameters achieved the mixing. The mixer was wetted by adding 2wt% of acetone. Uniaxial compacting via double action molds was carried out on electro hydraulic compacting machine type (Channel automatic cube and cylinder compression machines, CT340-CT440, UK). Two types of samples were prepared. Cylindrical of 10mm diameter and 5mm height used for hardness, microstructure, X-Ray, and machining tests, and the other is also cylindrical but with a diameter of 10mm and a height of 12mm used for compression test based on ASTM B925-08. The compacting pressure was determined experimentally based on presence of cracks on the surface of green compacts and by determining the pressure that gave the greatest green density. A loading rate of (0.3 kN/sec) was used for all compacting processes with duration of (30 sec) at the achieved pressure. Lubricant was used to the inside walls of the molds. Figure 2 shows the effect of compacting pressure on the green density of the compact samples. As it is obvious, there is an increase in the green density with the compacting pressure until a relatively constant value. Up on these results a compacting pressure of 900MPa was used to prepare the samples of this investigation. Samples were sintered according to the sintering program shown in Figure 3 via a vacuum furnace (GSL-1600x) with a pressure of 10^{-4} torrs.

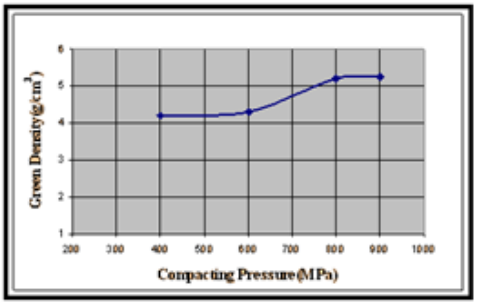

Figure 2. Effect of compacting pressure on green density of the prepared sample

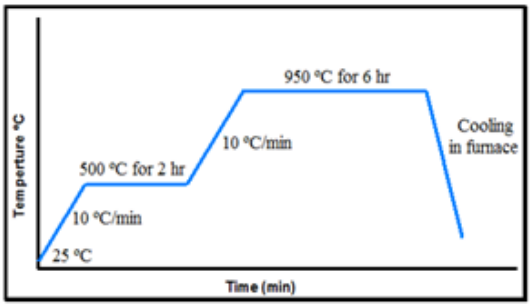

Figure 3. Sintering program of the prepared sample

4. SPECIMENS TESTS:

4.1. X-Ray diffraction:

The XRD was used to define the phases of sintered samples. The X - ray generator with Cu at 40 kV and 30 mA was used. A scanning speed of 7° (2θ) per minute was used. The detector was moved through an angle of 2θ = 20 to 80 degrees. Figure 4 represents the chart of x-ray diffraction results after sintering process of the alloy sample. The full transforming of NiTi alloy to monoclinic NiTi phase, cubic NiTi phase and hexagonal Ni_3Ti phase can be easily observed. The suggested reactions during the process are as following [13]:

$$Ni + Ti \rightarrow NiTi \qquad \Delta G: -67\ KJ/mol \ldots\ldots\ldots\ldots (1)$$
$$Ni + Ti \rightarrow Ni_3Ti \qquad \Delta G: -140\ KJ/mol \ldots\ldots\ldots\ldots (2)$$

According to the phase diagram of NiTi system, NiTi and Ni_3Ti are stable compounds, also reaction according to Eq.2 is more thermodynamically favored than that represented by Eq.1. Consequently, it is difficult to remove the Ni_3Ti from sintered sample only by altering the sintering condition [13, 14].

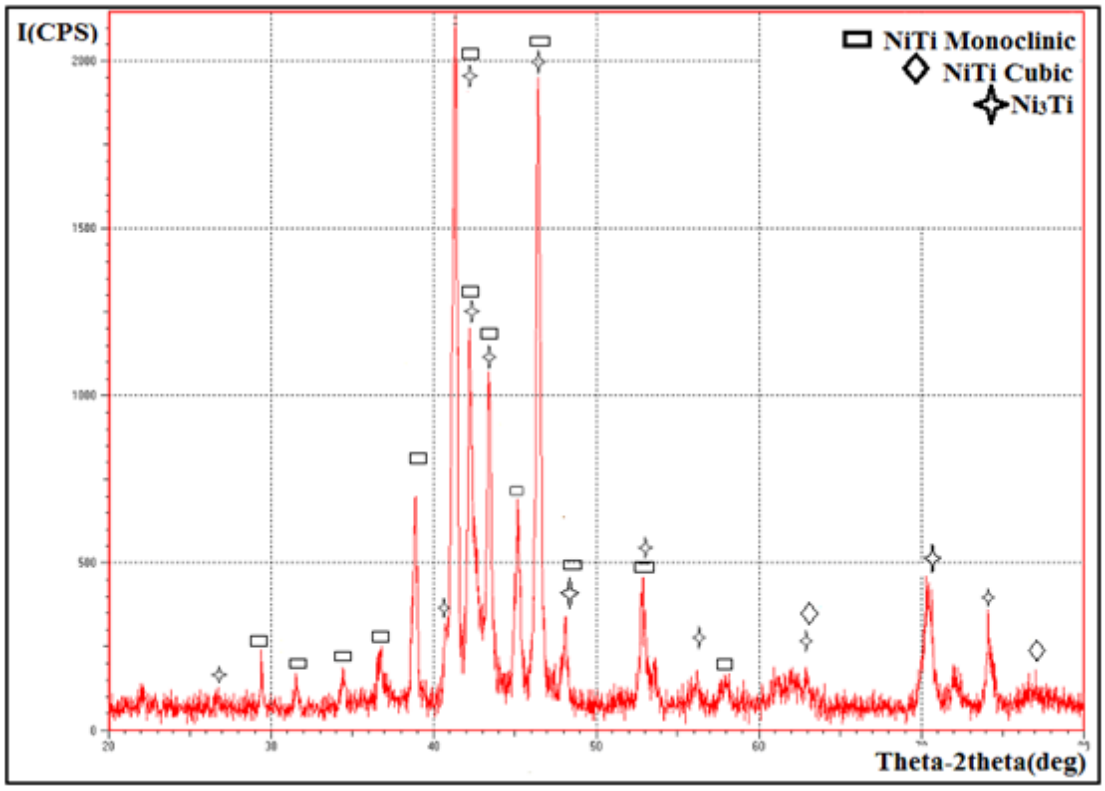

Figure 4. XRD Pattern of Sample after Sintering

4.2. Optical microscope (OM) and scanning electron microscope (SEM) tests:
The surfaces of the samples were wet ground using 120, 220, 320, 600, 1000, 1200 and 2000, grit silicon carbide papers. Etching solution consisting of [10% of HF, 20% of HNO_3 and 70% of H_2O] at room temperature was used [15]. The samples were washed with distilled water and dried using electric drier. Figure (5a) shows the microstructure of the sintered sample. Some features of the surface such as pores, grain boundaries, the phases NiTi and Ni_3Ti are clearly noticed. The pores are small and rarely interconnected. SEM image of the sample is shown in Figure(5b). The microstructure of sintered samples showed two kinds of phases also (NiTi and Ni_3Ti). The formation of martensite phase from disorder or ordered B2 (austenite) in the sintered sample is clearly.

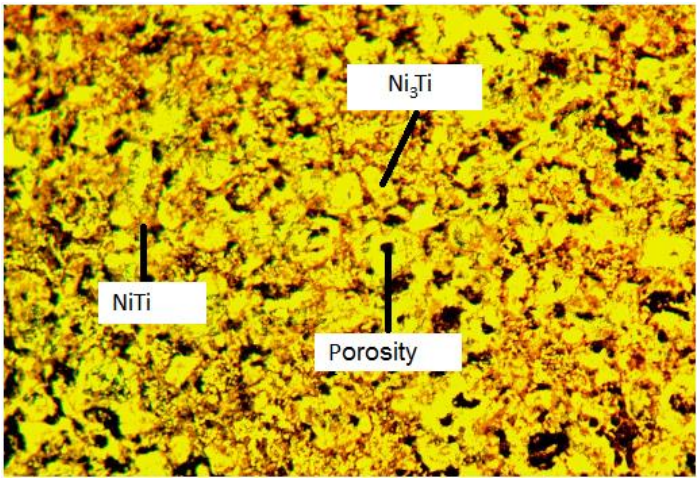

(a)

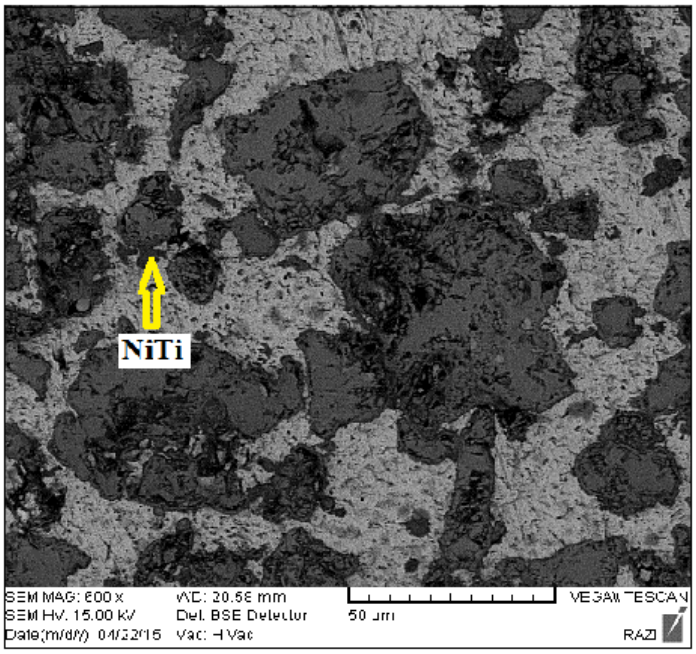

(b)

Figure 5. Microstructure of Sintered Alloy: (a) Optical (400x); (b) SEM Image

4.3. Mechanical Tests

Macro hardness Brinell's tester was used to measure the hardness of the sintered samples according to ASTM E10. A spherical indentation of 2.5mm diameter and a load of (31.25N) were used. An average of three readings had been recorded in this test.

The compression test was performed according to ASTM B925-08 specifications via universal testing machine type (WDW 200, china). The test was achieved at constant loading speed of 0.1mm/min.

The Shape memory effect (SME%) was determined based on Brinell's indentation as follows:

$$SME\% = \frac{d_b - d_a}{d_b} * 100 \quad \ldots\ldots\ldots\ldots\ldots\ldots\ldots\ldots\ldots (3)$$

Where: d_b= average impression diameter in (µm) before heating to 80°C, and d_a = average impression diameter in (µm) after heating to 80°C.

The tests showed that the hardness, compressive strength, and the shape memory effect are 137kg/mm^2, 431MPa, and 5.5% respectively. The results are in agreement with [16].

5. Chemical Machining Program:

Cylindrical samples of 10mm diameter and 5mm height were used in this test. Before coating with maskant material, the surface of sintered samples was ground by using (180,220,320,400,600,800 and 1000) grit silicon carbide papers, then rinsed by distilled water, dried by electric drying and wash with alcohol (ethanol 98%) and finally dried with air. A specially designed polymeric mold was used for coating the samples. The sample was placed inside the mold, then the polymeric maskant material (polyester) was poured, and only one side (face) of a sample was left without coating to be the area for chemical machining. Figure 6 shows sample after the coating. In this process 200ml of solution consisting of HCl, HNO_3 , and H_2O with concentration of 6%, 19%, and 75% respectively was used.

Figure 6. Specimens after coating

The machining process was achieved via magnetic stirrer thermostat. It contains a thermostat to regulate the temperature of etchant during the machining operation and controller on velocity of stirrer. Design of experiments via Taguchi method and L25 (2×5) mixed orthogonal array is utilized for the parametric design. Table (1) demonstrates the studied parameters with their levels for conducting the machining experiments.

Table 1. The Studied Parameters, Values and Levels

Parameter	Symbol	Unit	Level (1)	Level (2)	Level (3)	Level (4)	Level (5)
Machining Time	t_m	min	2	4	6	8	10
Machining Temperature	T	^{0}C	25	35	45	55	65

The "signal" to "noise" ratio, S/N, in decibels is used to determine the effect of the studied parameters on the response parameters. A category of "smaller is better" is used as the S/N ratio characteristic for the surface roughness, while a category of "greater is better" is used as the S/N ratio characteristic for the metal removal rate . These categories are expressed as following [17, 18]**:**

$$\frac{S}{N} = -10log_{10}\left[\frac{1}{n}\sum_{i=1}^{n}\left(y_i^2\right)\right]; i = 1,2,\ldots.,n \quad \ldots\ldots\ldots\ldots\ldots\ldots\ldots (4)$$

$$\frac{S}{N} = -10log_{10}\left[\frac{1}{n}\sum_{i=1}^{n}\left(1/y_i^2\right)\right]; i = 1,2,\ldots.,n \quad \ldots\ldots\ldots\ldots\ldots\ldots\ldots(5)$$

where *n* the number of observations, and y the observed data of the characteristic.
After each machining process, the specimen was taken out of the etchant solution, rinsed with water, dried with air dryer, washed with alcohol and dried with air dryer again. For each experiment, the surface roughness, weight loss and the metal removal rate were recorded. The weight was measured via sensitive weighing balance with an accuracy of (±0.0001).

6. Results and Discussion:

6.1. Results of the Machining Experiments:

Table (2) demonstrates the results of the machining experiments conducted according to Taguchi L25 (2×5) orthogonal array. Three readings for the response characteristic, Ra, and MRR had been recorded and their average value was considered. Taguchi design analyses and its details are shown in Figure 7 and Figure 8 for Ra and MRR respectively.

Table 2. Results of the Machining Experiments Conducted According to Taguchi L25 (2×5) Orthogonal Array

No.	t_m (min)	T (^{0}C)	Exp. Ra (μm)	Predicted Ra (μm)	Exp. MRR (g/min)	Predicted MRR (g/min)
1	1	1	0.27	0.264	0.0013	0.00136
2	1	2	0.37	0.388	0.0017	0.00177
3	1	3	0.52	0.496	0.0023	0.00236
4	1	4	0.55	0.588	0.0031	0.00314
5	1	5	0.68	0.666	0.0048	0.00409
6	2	1	0.31	0.291	0.0012	0.00115
7	2	2	0.42	0.430	0.0016	0.00152
8	2	3	0.58	0.554	0.0021	0.00207
9	2	4	0.7	0.662	0.0025	0.00280
10	2	5	0.72	0.754	0.0034	0.00370
11	3	1	0.34	0.336	0.0010	0.00110
12	3	2	0.44	0.491	0.0015	0.00143
13	3	3	0.64	0.630	0.0018	0.00193
14	3	4	0.79	0.753	0.0022	0.00262
15	3	5	0.84	0.861	0.0027	0.00348
16	4	1	0.43	0.4	0.0014	0.00122
17	4	2	0.47	0.569	0.0021	0.00150
18	4	3	0.74	0.724	0.0025	0.00196
19	4	4	0.89	0.863	0.0030	0.00260
20	4	5	1.01	0.986	0.0040	0.00341
21	5	1	0.51	0.481	0.0012	0.00149
22	5	2	0.66	0.666	0.0015	0.00172
23	5	3	0.81	0.836	0.0019	0.00214
24	5	4	1.05	0.99	0.0025	0.00274
25	5	5	1.08	1.129	0.0036	0.00351

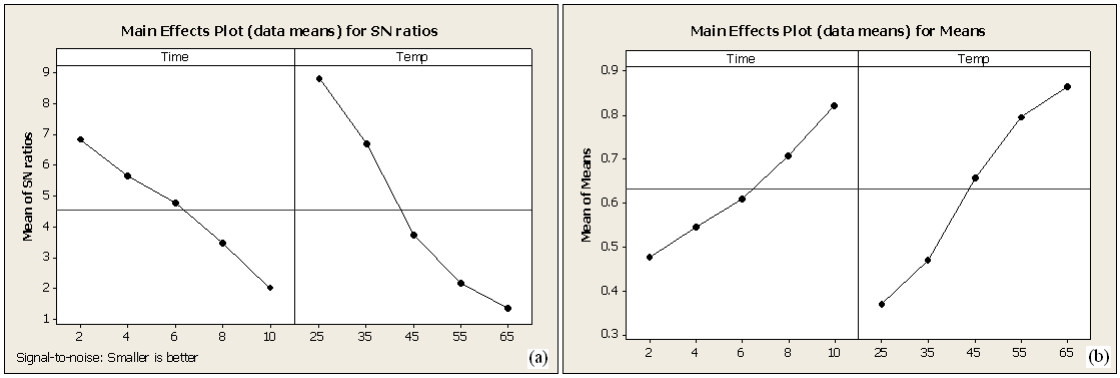

Figure 7. Results of Taguchi Design Analysis the Main Effect Plot for: (a) S/N Ratios; and (b) Surface Roughness

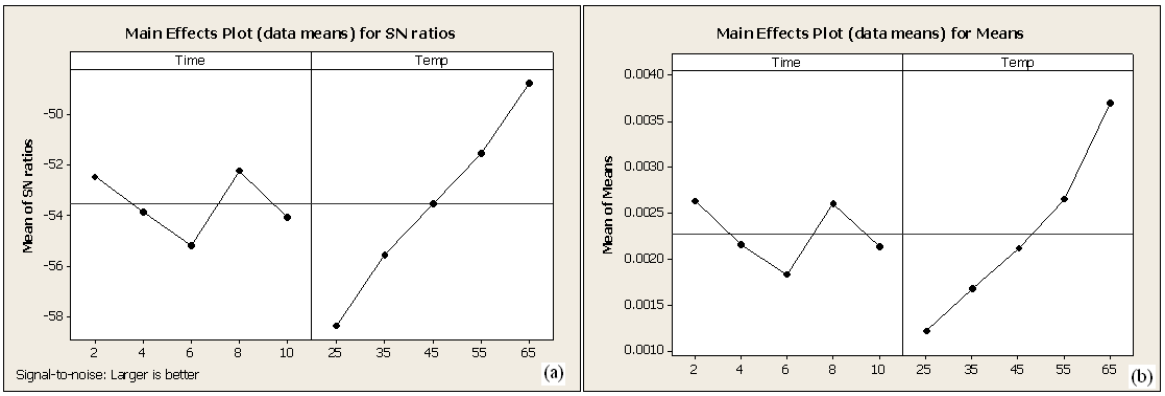

Figure 8. Results of Taguchi Design Analysis the Main Effect Plot of : (a) S/N Ratios ;and (b) the Metal Removal Rate

Figures 7&8 indicates that the machining temperature is the most significant factor, which controls both the surface roughness and the metal removal rate. A regression models were developed for predicting the surface roughness and the metal removal rate under various machining conditions using Datafit (Version 9.1) software. A various linear, exponential, power function and non-linear quadratic polynomial equations were examined in order to determine mathematical models which actually express on these parameters. The determination was based on the value of coefficient of multiple determination (R^2). It was found that non-linear quadratic polynomial equation has the maximum coefficient of multiple determination (R^2 = 0.976 and 0.86 for the models of Ra and MRR respectively). The regression models for Ra and for MRR are:

$$Ra = -0.0824 - 0.0191 * t_m + 0.01544 * T + 0.00225 * t_m^2 - 7.714 * 10^{-5} * T^2 + 7.7 * 10^{-4} * t_m * T \quad \text{..... (6)}$$

$$MRR = 0.00137 - 1.69 * 10^{-4} * t_m - 8.4 * 10^{-6} * T + 2 * 10^{-5} * t_m^2 - 9 * 10^{-7} * T^2 - 2.2 * 10^{-6} * t_m * T \quad \text{..... (7)}$$

The above models can be used to predict the metal removal rate and the surface roughness for any collection of the machining temperature, and the machining time within the range of the conducted experiments. Figure 9 shows the matching between the experimental values of Ra and MRR and their predicted values using the designed models respectively. This figure indicates that the developed models are capable to representing the system under the given experimental domain.

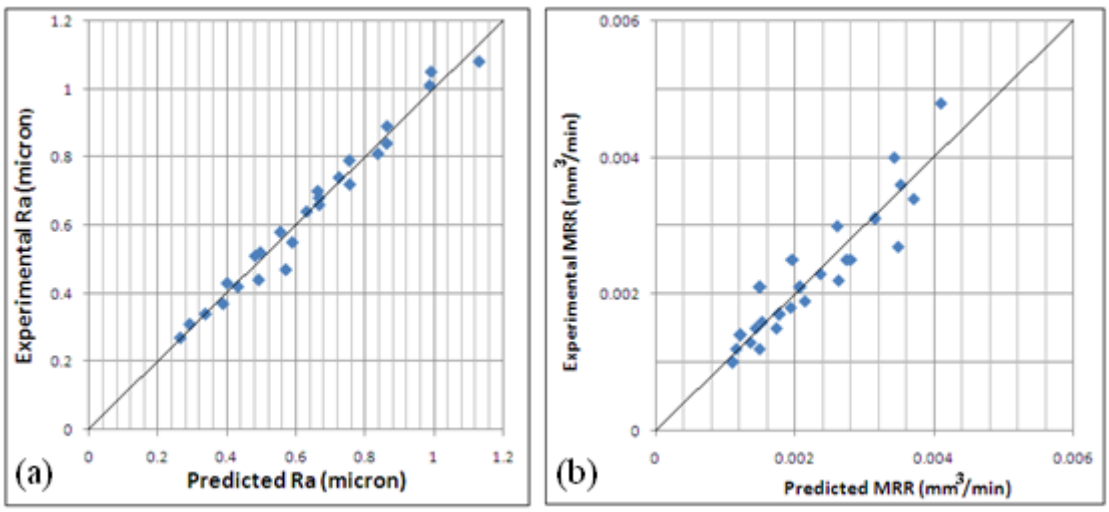

Figure 9. Scatter plot of the experimental and predicted values of: (a) Ra, and (b) MRR

Figure 10 show the effect of the machining temperature and machining time on the surface roughness, while Figure 11 shows the effect of these parameters on the metal removal rate.

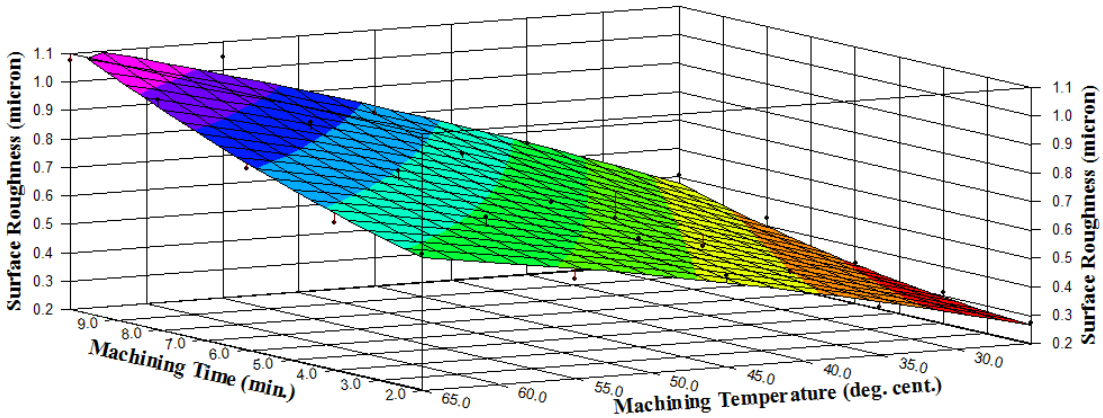

Figure 10. The Effect of Machining Temperature and Machining Time on Surface Roughness

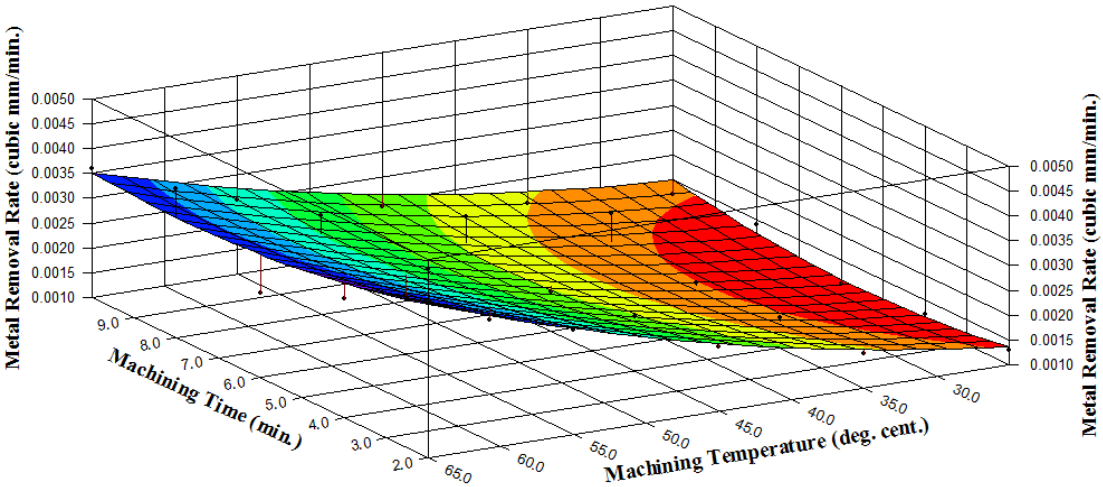

Figure 11. Effect of Machining Temperature and Machining Time on the Metal Removal Rate

6.2. Optimization of the Process Parameters:

A best set of optimum input parametric combinations resulting in a most desirable compromise between the responses (Ra and MRR) was determined based on desirability function via Mtb14.Table(3) demonstrates the key parameters set to find their global optimum setting.

Table 3. The key parameters set for optimization

Parameter	Goal	Target	Upper	Lower
MRR (g/min)	max.	0.00409	0.00409	0.0011
Ra (μm)	min.	0.264	1.129	0.264

The optimization results shown in Figure 12 indicates that a machining time for 2min in a temperature of 65^0C will give a minimum surface roughness with a maximum MRR. The individual desirability of MRR, and Ra are 1.0 and 0.535 respectively,while the composite desirability is 0.7314, which is a satisfactory value. A confirmation experiment was carried out to validate the resulted optimum

machining conditions. A comparison of the experimental Ra and MRR with their predicted values using optimal machining conditions indicates that the error percentage is 2% for the surface roughness and 14% for metal removal rate.

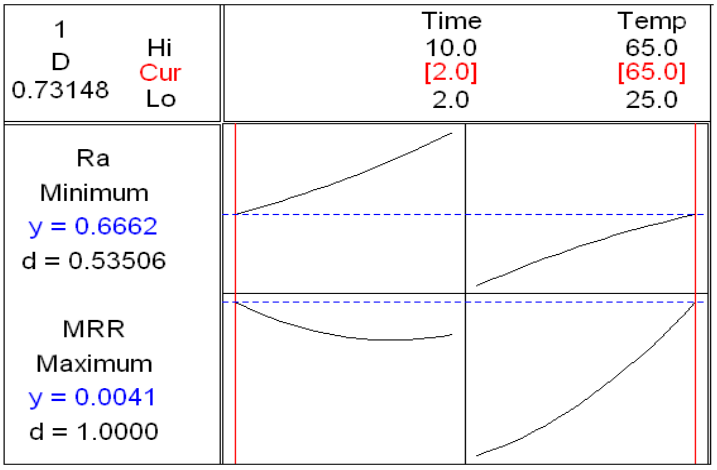

Figure 12. Optimization Results

7. Conclusions

Based on the results obtained in the present work, the conclusions can be summarized as follows:

1- Mechanical and physical tests indicated that NiTi SMA alloy can be produced by PM using compacting pressure of 900MPa and sintering at 950^0C for 6hrs.

2- Machining temperature and machining time have significant effects on the surface roughness and the producibility of chemical machining of the NiTi SMA alloy, but the machining temperature is the most significant factor, which controls both the surface roughness and the metal removal rate.

3. A minimum surface roughness of 0.666µm with a maximum metal removal rate of 0.0041g/min can be associated with a machining temperature of 65^0C and machining time of 2min.

References

[1] Tan L. and Cron W. C. 2004 'In Situ TEM Observation of Two - Step Martensitic Transformation in Aged NiTi Shape Memory Alloy', *Script a material*, **50**, PP (819 – 823).

[2] Dimities La Goudas 2008 '*Shape Memory Alloys Modeling and Engineering Application*', Texas A&M University, USA.

[3] Lee Eun Sang, and Shin Tae Hee 2011 'An Evaluation of the Machinability of Nitinol Shape Memory Alloy by Electrochemical Polishing', *Journal of Mechanical Science and Technology* **25** (4), PP (963-969).

[4] Weinert K., Petzoldt V. 2004 'Machining of NiTi Based Shape Memory Alloys', *Materials Science and Engineering A* **378**, PP (180–184).

[5] Mehrshad Mehrpouya , Abed Moheb Shahedin, Sarmad Daood Salman Dawood & Ahmad Kamal Ariffin 2017 'An investigation on the optimum machinability of NiTi based shape memory alloy', *Materials and manufacturing processes* **32**(13).

[6] Huang H, Zhang H, Zhou L and Zheng H Y 2003 'Ultrasonic Vibration Assisted Electro-Discharge Machining of Microholes in Nitinol' *Journal of Micromechanics and Microengineering* **13**, PP (693–700).

[7] Chengde Li, Suwas Nikumb, Franklin Wong 2006 'An Optimal Process of Femtosecond Laser Cutting of NiTi Shape Memory Alloy for Fabrication of Miniature Devices', *Optics and Lasers in Engineering* **44**, PP (1078–1087).

[8] Pfeifer Ronny ∗, Herzog Dirk, Hustedt Michael, Barcikowski Stephan 2010 'Pulsed Nd:YAG Laser Cutting of NiTi Shape Memory Alloys—Influence of Process Parameters', *Journal of Materials Processing Technology*, **210**,PP (1918–1925).

[9] Muhammad N., Whitehead D., Boor A., Oppenlander W., Liu Z., Li L. 2012 'Picosecond Laser Micromachining of Nitinol and Platinum–Iridium Alloy for Coronary Stent Applications', *Applid Physics A* 106, pp. (607–617).

[10] Abidi Mustufa Haider, Abdulrahman M. Al-Ahmari, Arshad Noor Siddiquee, Syed Hammad Mian , Muneer Khan Mohammed and Mohammed Sarvar Rasheed 2017 'An Investigation of the Micro-Electrical Discharge Machining of Nickel-Titanium Shape Memory Alloy Using Grey Relations Coupled with Principal Component Analysis', *Metals* **7** (486).

[11] El-Hofy, H. A. G 2005 '*Advanced Machining Processes*', McGraw-Hill Companies OH USA.

[12] Al-Ethari Haydar A. H., Alsultani Kadhim Finteel, Nesreen Dakhel F. (2014) 'Optimization of Chemical Machining Conditions of Cold Worked Stainless Steel 420 Using Taguchi Method', *International Journal of Mechanical Engineering and Technology*, **5**(3), PP (57-65).

[13] Zhu S.L., Yang X.J., Fu D.H., Zhang L.Y., Li C.Y. and Cui Z.D. 2005 'Stress-Strain Behavior of Porous NiTi Alloys Prepared by Powder Sintering', *Materials Science and Engineering* **A408**, PP (264-268).

[14] Bing-Yun Li, Li-Jian Rong, Yi-Yi Li and Gjunter V. E. 2000 'An Investigation of The Synthesis of Ti-50 At. Pct Ni Alloys Through Combustion Synthesis and Conventional Powder Sintering', *Metallurgical and Materials Transactions A*, **31A** (7), PP (1867-1871).

[15] Jafari J., Zebarjad S. and Sajjadi S. 2008 'Effect of Pre - strain on Microstructure of Ni - Ti Orthodontic Arch Wires', *Materials Science and engineering A*. **473**, PP (42 – 48).

[16] Dawood N.M. 2014 '*Preparation and Characterization of Bio Nitinol with Addition of Copper*', *PhD. thesis*, Materials Engineering Department, University of Technology/ Iraq.

[17] Mali Harlal Singh, Manna Alakesh 2010 'Optimum Slection of Abrasive Flow Machining Conditions During Fine Finishing of Al/15 wt% SiC-MMC Using Taguchi Method, *International Journal of Advance Manufacturing Technology*, **50**, PP (1013–1024).

[18] Babu Rao. J, Venkata Rao.D. and Bhargava 2010 'Development of Light Weight Alfa Composites', *International Journal of Engineering, Science and Technology*, **2** (11), PP (50-59).